

Protein Adsorption on Nano-scaled, Rippled TiO₂ and Si Surfaces

Jana Sommerfeld · Jessica Richter ·
Raphael Niepelt · Stefanie Kosan · Thomas F. Keller ·
Klaus D. Jandt · Carsten Ronning

Received: 12 July 2012 / Accepted: 13 August 2012 / Published online: 7 September 2012
© The Author(s) 2012. This article is published with open access at Springerlink.com

Abstract We synthesized nano-scaled periodic ripple patterns on silicon and titanium dioxide (TiO₂) surfaces by xenon ion irradiation, and performed adsorption experiments with human plasma fibrinogen (HPF) on such surfaces as a function of the ripple wavelength. Atomic force microscopy showed the adsorption of HPF in mostly globular conformation on crystalline and amorphous flat Si surfaces as well as on nano-structured Si with long ripple wavelengths. For short ripple wavelengths the proteins seem to adsorb in a stretched formation and align across or along the ripples. In contrast to that, the proteins adsorb in a globular assembly on flat and long-wavelength rippled TiO₂, but no adsorbed proteins could be observed on TiO₂ with short ripple wavelengths due to a decrease of the adsorption energy caused by surface curvature. Consequently, the adsorption behavior of HPF can be tuned on biomedically interesting materials by introducing a nano-sized morphology while not modifying the stoichiometry/chemistry.

1 Introduction

The acceptance of artificial replacements is chiefly determined by cell and platelet adsorption out of the surrounding human environment. This in turn is mediated by protein adsorption on the surface of the corresponding device [1–3]. An improvement and acceleration of the healing after surgical intervention would cause a tremendous enhancement of life quality. Therefore, finding optimized functional materials that are able to attract or repel specific molecules is recently in a strong focus of life sciences [4–6]. Thus, the question arises how one can improve and modify the interface between a specific material and its biological surrounding by subsequent physical treatments, e.g. such as ion, laser, or electron irradiation.

A general understanding of the mechanisms involved in protein adsorption can be gained by investigating human plasma fibrinogen (HPF) on surfaces, because of its importance for the blood coagulation process and the fact that its structure is well known [1, 7, 8]. Most notably, HPF has an amphiphilic character that causes its hydrophobic and hydrophilic parts to be attracted to hydrophobic and hydrophilic surfaces, respectively, assuming different conformations. As can be seen in Fig. 1a, the structure of HPF consists of two hydrophobic domains, E and D, which are built up of individual amino acids. At the outer ends of the protein are carboxyl groups (α chains) with a hydrophilic character [9]. Hence, it is possible for HPF to undergo conformational changes depending on the environmental conditions. According to the experimental findings by Marchin and Berrie [10], the hydrophobic domains preferentially adsorb on hydrophobic surfaces. Owing to the ambition of each domain to connect with the surface, HPF finally adsorbs in a stretched formation as is illustrated in Fig. 1b. On the other hand, the attraction of

J. Sommerfeld, J. Richter and R. Niepelt contributed equally to this manuscript.

Electronic supplementary material The online version of this article (doi:10.1007/s13758-012-0055-5) contains supplementary material, which is available to authorized users.

J. Sommerfeld (✉) · J. Richter · R. Niepelt · S. Kosan ·
C. Ronning
Institute of Solid State Physics, Friedrich Schiller University,
Helmholtzweg 3, 07743 Jena, Germany
e-mail: jana.sommerfeld@uni-jena.de

T. F. Keller · K. D. Jandt
Institute of Materials Science and Technology (IMT), Friedrich
Schiller University, Löbdergraben 32, 07743 Jena, Germany

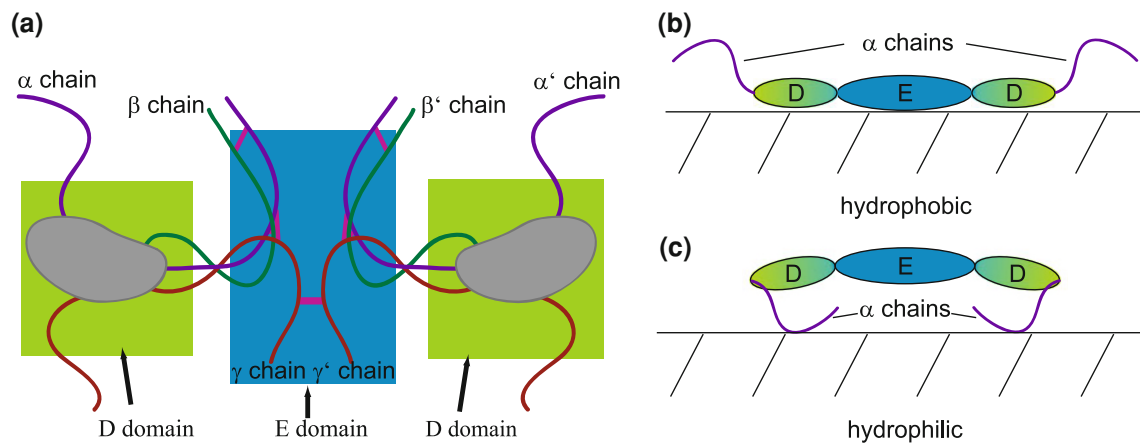


Fig. 1 **a** Schematic sketch of the HPF molecule. The hydrophobic E and D domains consist of amino acids; whereas, its hydrophilic α chains at the outer ends are based on carboxyl groups. This structural combination allows a conformational change after the adoption on a material: **b** on hydrophobic surfaces, the hydrophobic domains D and

E preferentially adsorb, which results in a stretched conformation. **c** The hydrophilic α chains are more attracted to hydrophilic surfaces. The chains interfold for the latter case in order to improve the connection, which leads to a rather globular structure

the hydrophilic α chains to the surface dominates on hydrophilic surfaces. The α chains “fold” underneath the E and D domains resulting in a more globular conformation (see Fig. 1c). Surface-bonded HPF has a length of 46–49 nm and a height about 0.3–2.5 nm depending on the protein conformation on different substrates and under different environmental conditions [7, 10–13]. Former studies mostly investigated the adsorption of HPF and a variety of other proteins [14, 15] on flat substrates such as commercially pure Ti with a natural TiO_2 layer on top [13], TiO_2 [7], graphite [10, 11, 16], mica [10, 12, 13], ultra-high molecular weight polyethylene [17], Si [18] or SiO_2 [19]. In most cases, these investigations concentrated on the adsorption of single proteins in air and/or under aqueous conditions. A general conclusion is that the adsorption behavior is mainly given by the chemistry of the surface. Cai et al. [20] in turn gave evidence that the surface roughness has little effect, while another study by Rasmusson et al. [21] links the formation of HPF to the curvature of the investigated surface. Thus, the influence of the surface morphology on the nanoscale seems to be minor as deduced from the previous studies for protein adsorption.

A controlled manipulation of the surface morphology can be realized by means of ion beam bombardment, which can be used to cause a periodical structure on a nanometer scale that matches the diameter of proteins. When an energetic ion hits a target, its entire energy is transferred to the target system. If the impact energy is high enough and the energy devolution takes place close to the surface, a fraction of target atoms nearest to the surface will be sputtered off the substrate. A detailed theory of the sputter process itself and the thereby caused roughening of the

surface was elaborated by Sigmund [22]. Due to self-diffusion of the surface atoms, a smoothing process can be observed. Finally, the interaction of the described roughening and smoothing causes periodical structures which are called ripples [23]. It was recently shown that osteoblasts show an enhanced response on ion beam irradiated, rippled titanium surfaces pointing to an effect of the ripple pattern on the cell attachment process [4].

Therefore, introducing morphological changes by means of ion beams offers a new approach to influence the adsorption behavior of proteins on established biomaterials without changing their surface chemistry. In this work, we concentrated on TiO_2 that is often used for artificial replacements as this material is well known for its non-toxic, biocompatible character. We investigated the adsorption behavior of HPF on TiO_2 as a function of the ripple wavelength and observed a clear influence of the nanostructure on the protein adsorption. Additionally, we performed the same experiments on rippled Si as a reference.

2 Structural Characterization

Both TiO_2 and Si $\langle 100 \rangle$ single crystal samples were irradiated with xenon ions with ion energies ranging from 5 to 20 keV in order to vary the wavelength of the created ripples. The angle between the surface and the incident ion beam was $70\text{--}72^\circ$ and typical ion fluences of 10^{16} ions/cm² (fluxes of $1 \mu\text{A}/\text{cm}^2$) were applied. Xenon ions exclude any doping effects on the substrate, as noble gas atoms do not form any bonds and mostly diffuse out rapidly after irradiation at room temperature. The inset of Fig. 2a

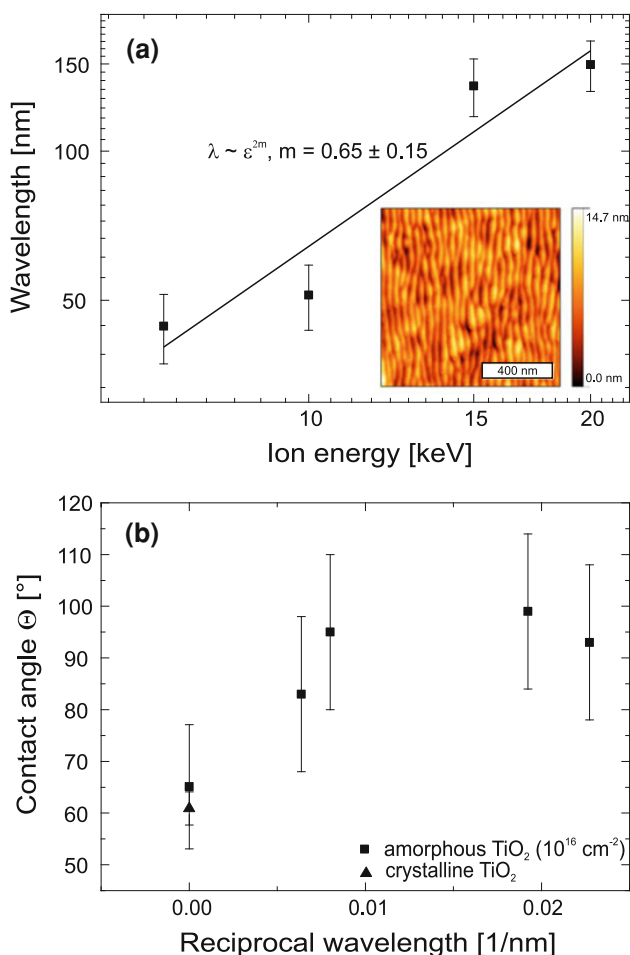


Fig. 2 **a** Wavelength dependency of the ripple pattern on the ion energy for TiO₂. The wavelength of the created ripples follows a power law dependence with increasing ion energy. The *inset* shows an AFM picture of TiO₂ irradiated with 7 keV Xe ions and an ion fluence of $3 \times 10^{16} \text{ cm}^{-2}$. **b** Contact angles of water on flat and rippled TiO₂ as a function of the reciprocal ripple wavelength. In comparison to non-irradiated and flat TiO₂ (*triangle*), the contact angle increases slightly from $60.9^\circ \pm 3.2^\circ$ to $65.1^\circ \pm 12.0^\circ$ for irradiated and flat TiO₂. The values for rippled TiO₂ exhibit larger error bars because of a smaller irradiation area in comparison to the flat TiO₂ that could be investigated

exemplarily shows an atomic force microscopy (AFM) picture of a TiO₂ surface irradiated with 7 keV Xe ions. The wavelength λ of the ripple pattern was determined by 2D autocorrelation and is plotted in Fig. 2a, showing a clear power law dependence with increasing ion energy ε : $\lambda \sim \varepsilon^{2m}$. We calculated a value for the exponent m of 0.65 ± 0.15 for TiO₂, which is above the value of $m = 0.3$ expected from the theory for ion-induced surface self-diffusion. However, the discrepancy can be explained by considering redeposition processes during the sputter process, which lead to a coarsening of the ripple wavelength over irradiation time [24, 25]. For our Si reference sample set we obtained an exponent m of 0.5 ± 0.05

(see supplementary information), which is well in agreement with experimental data already published [26], obtained from irradiation with argon ions.

Contact angle measurements (CAM) of water reveal that the contact angle Θ slightly but not significantly increases from $60.9^\circ \pm 3.2^\circ$ to $65.1^\circ \pm 12.0^\circ$ for flat TiO₂ after irradiation with xenon ions which had an energy of 20 keV. The fluence was $5 \times 10^{16} \text{ cm}^{-2}$ and the sample was irradiated under an incident ion beam angle of 0° to the surface normal. The same result was also found for flat silicon surfaces: no change of the contact angle after ion irradiation. Note, the latter is accompanied with an amorphization of the surface. However, changes of the hydrophobicity might occur with structural changes. Hence, Fig. 2b shows the obtained contact angles for rippled TiO₂ with different reciprocal wavelengths. Within the range of error, we found an increase of the contact angle, about 25–30°, for high wavelengths (small reciprocal wavelength) indicating an influence of the surface curvature on the surface chemistry. However, the contact angles remain unchanged within the range of error for small wavelengths (high reciprocal wavelengths). Therefore, we can exclude an influence of the ripple wavelength on the surface chemistry.

X-ray photoelectron spectroscopy (XPS) was performed on both non- and Xe-irradiated TiO₂ and Si surfaces (see supplementary information). The untreated TiO₂ samples show an excess of oxygen due to the coverage with adsorbed OH molecules over long periods in atmosphere that is decreased after ion beam irradiation. Nonetheless, the irradiated TiO₂ had a perfect stoichiometric surface even after weeks of exposure to air. In contrast, Si surfaces oxidize very fast in air and we observed the common oxygen features of SiO₂ [27], irrespective of performing ion irradiation or not.

Summarizing the part above, Xe ion irradiation induces a clear periodic nano-patterned ripple surface structure for both material systems. The structure can be tuned by the used ion energy. Nonetheless, Xe ion irradiation has only a negligible effect on the surface stoichiometry/chemistry. The latter was detected by both XPS and CAM investigations for flat surfaces. In any case, each set of TiO₂ and Si samples exhibits the same surface chemistry before and after the ion irradiation process. However, the ripples have an influence on the hydrophobicity.

3 Protein Adsorption

We observed that a dense film of fibrinogen is adsorbed in apparently globular conformation (compare to Fig. 1) on top of flat, non-irradiated TiO₂, as shown in Fig. 3a, as well as on flat, irradiated TiO₂ (Fig. 3b). Both pictures do not reveal any networks of the adsorbed HPF, which indicates

that it was not possible for the α chains to interact. Thus, we assume that the α chains attach to the surface and shield the hydrophobic D and E domains which are piling up on top (see Fig. 1c) resulting in a globular assembly of HPF. This adsorption behavior was also observed for single proteins on Ti with TiO₂ surfaces [13]. On non-irradiated and irradiated flat Si we observed mostly globularly adsorbed proteins with small amount of HPF networks (see supplementary information). The latter probably originates from some proteins that adsorb in a stretched conformation, which is well in agreement with the hydrophilic character of the SiO₂ layer on top of Si [19].

Figure 4a shows an AFM height picture of TiO₂ with a ripple wavelength of $\lambda = 125$ nm after the adsorption process. The markings indicate some of the proteins that adsorb in globular conformation. The AFM height picture of TiO₂ with a shorter ripple wavelength of $\lambda = 52$ nm after the protein adsorption process is shown in Fig. 4b, which equals the measurements before the adsorption

process. Consequently, for wavelengths of $\lambda = 52$ nm and $\lambda = 44$ nm (not shown here) we could not detect any adsorbed proteins.

In Fig. 5 an overview of the AFM measurements is given for Si with varying ripple wavelengths after the protein adsorption. On the left side of Fig. 5, the AFM height images give information concerning the possible conformation of the proteins. The continuous lines through the images indicate the position of the taken cross section measurements, to be seen on the right side of Fig. 5. It is clearly visible that the backbones of the ripples have an irregular shape, which is caused by the adsorbed proteins. A globular conformation of the adsorbed proteins, which is comparable to the situation for flat surfaces, is observed for ripple structures with a long wavelength ($\lambda = 146$ nm), as shown in Fig. 5a, b. Thus, “smooth” morphology compared to the size of the proteins has no influence on the adsorption behavior, as one can expect. Significant changes appear when the ripple wavelength is as low as about

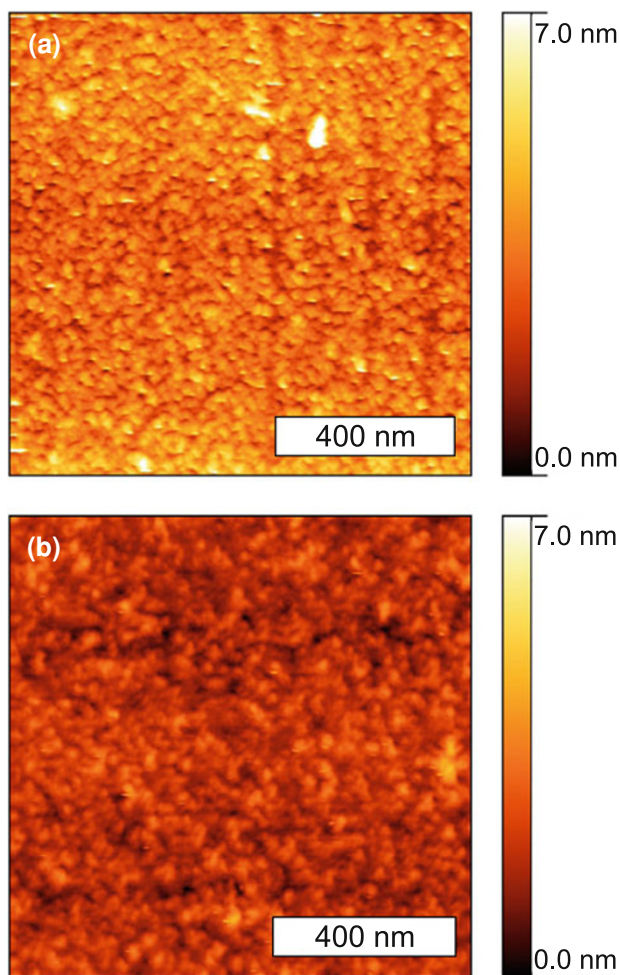


Fig. 3 AFM height pictures of adsorbed HPF on **a** non-irradiated and **b** irradiated flat TiO₂. A dense HPF film adsorbs with no resolved networks of the protein molecules in globular conformation

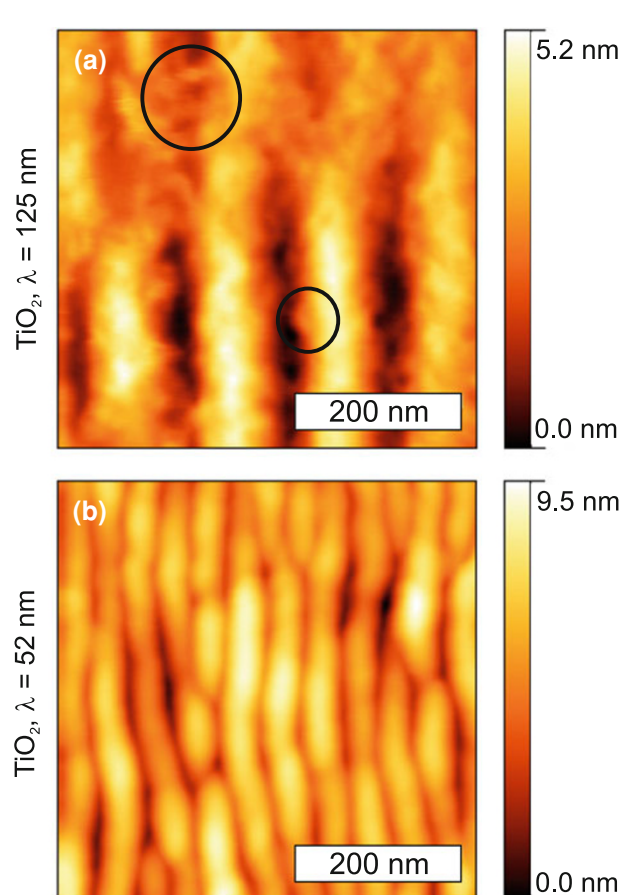


Fig. 4 AFM images of TiO₂ with rippled surfaces of wavelengths **a** $\lambda = 125$ nm and **b** $\lambda = 52$ nm after protein adsorption. The adsorbed proteins are clearly seen (*markings*) and seem to be assembled in globular conformation for long wavelength samples, while proteins could not be observed for smaller wavelengths by AFM

$\lambda = 68$ nm (see Fig. 5c, d). The fibrinogen molecules adsorbed in a stretched conformation, apparently parallel to the orientation of the ripples. Decreasing the ripple wavelength even more down to $\lambda = 52$ nm (Fig. 5e, f) leads to a perpendicular orientation of HPF to the ripple backbones

on Si. Moreover, it seems that adsorption on rippled Si only took place on top of the hillocks, never in the valley. This presumption is based on the fact that in the case of protein adsorption, an increase of about 1.1–1.6 nm of the ripple amplitudes was detected, which is in the range of the

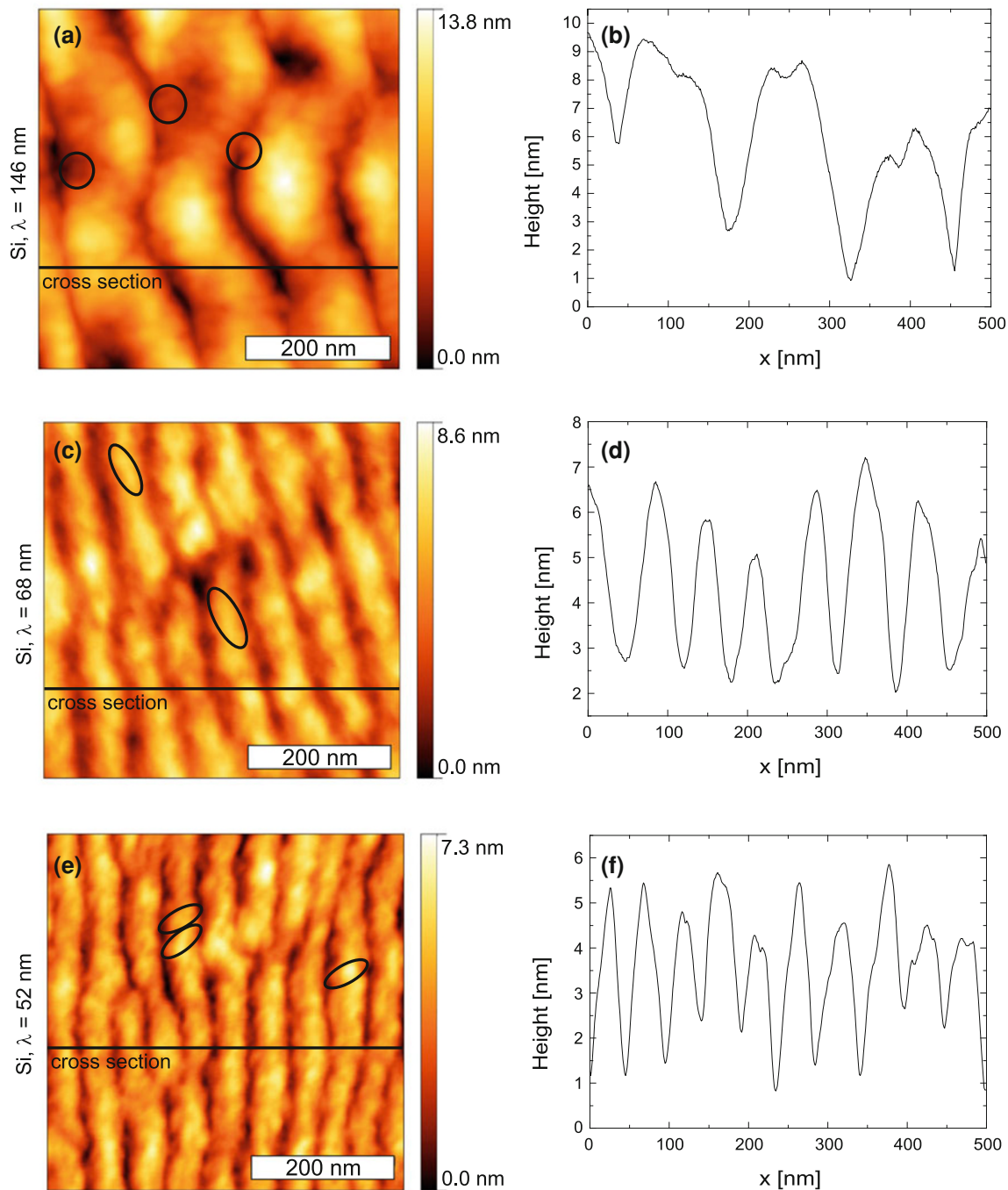


Fig. 5 AFM analysis of rippled Si with varying wavelengths after protein adsorption and the corresponding cross sections along the continuous line. HPF adsorbed in a globular conformation for long ($\lambda = 146$ nm) wavelength Si ripples (a, b). For a shorter wavelength ($\lambda = 68$ nm) of the Si ripples, HPF adsorbed in a stretched

conformation along the ripple backbones (c, d). For the shortest wavelength investigated ($\lambda = 52$ nm), the HPF still adsorbed in stretched conformation but with an orientation across the ripple backbones (e, f)

protein height. In the case of protein attachment only in the valleys or spread over the entire area, a decrease or no change at all of the amplitude should have occurred, which was not the case.

We used HPF concentrations (see supplementary information) that were sufficient for a full surface coverage, so that the molecules can connect with each other, as shown for the flat Si or TiO₂ substrates. End-to-end interactions of the proteins finally lead to weakly bonded protein networks in the case of the Si substrate. When introducing a nanostructure on a surface, the protein networks cannot muster stable bindings. The adsorption of single proteins on ripple structures with long wavelengths ($\lambda > 100$ nm) seems to rely basically on the surface chemistry. In our case, this resulted in a globular conformation of HPF molecules with folded α chains underneath the domains, which is in good agreement with the investigations of Van de Keere et al. [13] on Ti substrates with TiO₂ surfaces and Tunc et al. [28] on SiO₂. Based on the theoretical findings of Melis et al. [29] for the adsorption of synthetic oligomers, the adhesion of the proteins on our nano-rippled surfaces might be decreased when a curvature appears that is within the size of the protein. Hence, we presume that by increasing the surface curvature (smaller wavelength) for Si, the adsorption energy is decreased. Therefore, it is energetically favorable for the proteins to stretch. By doing this, the contact area between substrate and protein is increased assuring adsorption. This theory accords well with the findings by Rasmusson et al. [21] and Roach et al. [30] for the adsorption of HPF on polymer nanostructures and silica nanospheres, for example. The dependence of the orientation of the proteins on the ripple wavelength can be explained as follows. For large wavelengths, the adsorption takes place along the ripple backbones. The situation changes when the wavelength is decreased and thus the curvature is increased. In this case, the required optimization of the adsorption energy is only possible by additional protein–protein interaction. This eventually results in an alignment of the proteins across the ripple backbones, which increases the contact area between neighboring proteins. Protein–protein interaction leading to an increased surface coverage is also described by Roach et al. [3]. Although we observed the described adsorption behavior on short-wavelength ripples only on Si surfaces, we assume a similar effect for TiO₂. However, we could not observe any adsorbed proteins on short-wavelength TiO₂ ripples, which might be caused by the fact that the adsorption energy of TiO₂ is even more decreased than the one of Si. Thus, the adsorption energy was not sufficient for the proteins to attach or to withstand the rinsing procedure. Taking into account that after the adsorption of proteins the samples were rinsed and assuming a small binding energy of short-rippled TiO₂, weakly bound

proteins on the surface were likely to be removed during the preparation process.

As a consequence, the adsorption behavior of HPF does not seem to rely exclusively on the surface chemistry. A change of the substrate morphology has a major effect on the protein attachment to a substrate. This theory is further supported by the fact that we found an increased water contact angle for TiO₂ with short wavelengths, which therefore has a more hydrophobic character. According to the findings by other groups [12, 28], HPF should adsorb more strongly on this hydrophobic surfaces because of the chemistry of the surface. Since this was not the case, we interpret the fact that we did not observe proteins to be a result of the local surface curvature. In order to explain the observation that proteins only adsorbed on the ridges of the ripples, we like to propose the following model: Due to the experimental process, the proteins approach the range of the surface potential of the backbones first and start to adsorb there. According to Siegismund et al. [31], the migration probability for directions combining HPF molecules is higher than that for isolated molecules. Thus, adjacent proteins adsorb around the backbones as well, which finally leads to the coverage only on top of the ripple backbones.

4 Conclusions

By preparing nano-sized ripple structures on biomedically relevant materials such as TiO₂ and Si via ion beam bombardment, we investigated the influence of the nano-sized morphology on the adsorption behavior of HPF. We found that HPF adsorbs mostly in globular conformation on flat Si and TiO₂ surfaces. In the case of Si, some proteins seem also to adsorb in stretched conformation allowing the proteins to interact and cause little network structures. For long ripple wavelengths ($\lambda > 100$ nm), the globular adsorption is observed on both materials; whereas, a rather stretched fibrinogen conformation and alignment appeared on short-wavelength ($\lambda \approx 50$ nm) rippled Si. Adsorbed proteins were not found by AFM in the case of short-wavelength rippled TiO₂. The observation is mainly explained by a decrease of the adsorption energy due to surface curvature. Concluding, it is possible to tune the adsorption behavior of proteins on biomedical materials just by changing the morphology while not modifying the stoichiometry/chemistry.

Acknowledgments We thank Ralf Wagner of the Institute of Materials Science and Technology (University of Jena) for the XPS analysis. Furthermore, we thank Prof. Friedrich Huisken and the Laboratory Astrophysics and Cluster Physics group (University of Jena) for the use of their lab and equipment.

Open Access This article is distributed under the terms of the Creative Commons Attribution License which permits any use, distribution, and reproduction in any medium, provided the original author(s) and the source are credited.

References

1. Doolittle RF (1984) *Annu Rev Biochem* 53:195–229
2. Lindon J, McManama G, Kushner L, Merrill E, Salzman E (1986) *Blood* 68:355–362
3. Roach P, Farrar D, Perry CC (2005) *J Am Chem Soc* 127: 8168–8173
4. Riedel NA, Williams JD, Popat KC (2011) *J Mater Sci* 46: 6087–6095
5. Lord MS, Foss M, Besenbacher F (2010) *Nano Today* 5:66–78
6. Stupp SI (2010) *Nano Lett* 10:4783–4786
7. Cacciafesta P, Humphris LAD, Jandt KD, Miles MJ (2000) *Langmuir* 16(21):8167–8175
8. Hall CE, Slayter HS (1959) *J Biophysic Biochem Cytol* 5(1): 11–17
9. Feng L, Andrade JD (1995) *Proteins at Interfaces II: Fundamentals and Applications*; ACS Symposium Series 602; Chapter 5. American Chemical Society, USA
10. Marchin KL, Berrie CL (2003) *Langmuir* 19(23):9883–9888
11. Agnihotri A, Siedlecki CA (2004) *Langmuir* 20:8846–8852
12. Sit PS, Marchant RE (1999) *Thromb Haemost* 82:1053–1060
13. Van De Keere I, Willaert R, Hubin A, Vereecken J (2008) *Langmuir* 24:1844–1852
14. Vieira EP, Rocha S, Pereira MC, Möhwald H, Coelho MAN (2009) *Langmuir* 25(17):9879–9886
15. Kim J, Somorjai GA (2003) *J Am Chem Soc* 125:3150–3158
16. Ta TC, Sykes MT, McDermott MT (1998) *Langmuir* 14: 2435–2443
17. Keller TF, Schönfelder J, Reichert J, Tuccitto N, Licciardello A, Messina GML, Marletta G, Jandt KD (2011) *ACS Nano* 5(4): 3120–3131
18. Ortega-Vinuesa JL, Tengvall P, Lundström I (1998) *Thin Solid Films* 324:257–273
19. Jung SY, Lim SM, Albertorio F, Kim G, Gurau MC, Yang RD, Holden MA, Cremer PS (2003) *J Am Chem Soc* 125: 12782–12786
20. Cai K, Bossert J, Jandt KD (2006) *Colloids Surf B* 49:136–144
21. Rasmusson JR, Erlandson E, Salaneck WR, Schott M, Clark DT, Lundström I (1994) *Scanning Microsc* 8(3):481–490
22. Sigmund P (1969) *Phys Rev* 184(2):383–416
23. Bradley RM, Harper JME (1988) *J Vac Sci Technol A* 6(4): 2390–2395
24. Keller A, Facsko S (2010) *Materials* 3:4811–4841
25. Yewande EO, Hartmann AK, Kree R (2005) *Phys Rev B Condens Matter Mater Phys* 71:195405-1–195405-8
26. Chini TK, Datta DP, Bhattacharyya SR (2009) *J Phys Condens Matter* 21:224004
27. Nefedov VI, Salyn YV, Leonhardt G, Scheibe R (1977) *J Electron Spectrosc Relat Phenom* 10:121–124
28. Tunc S, Maitz MF, Steiner G, Vázquez L, Pham MT, Salzer R (2005) *Colloids Surf B* 42:219–225
29. Melis C, Mattoni A, Colombo L (2010) *J Phys Chem* 114: 3401–3406
30. Roach P, Farrar D, Perry CC (2006) *J Am Chem Soc* 128: 3939–3945
31. Siegismund D, Keller TF, Jandt KD, Rettenmayr M (2010) *Macromol Biosci* 10:1216–1223